ISSN 1070-3284, Russian Journal of Coordination Chemistry, 2022, Vol. 48, No. 8, pp. 526–535. © Pleiades Publishing, Ltd., 2022.

Soft N-Type Functionalized Fluorenyl Ligated Rare-Earth Metal Complexes: Synthesis, Structure, and Catalytic Performance for 2-Vinylpyridine

Z. H. Mou[a], * and Y. J. Wang[a]

[a] *Key Laboratory of Advanced Mass Spectrometry and Molecular Analysis of Zhejiang Province, School of Materials Science and Chemical Engineering, Ningbo University, Ningbo, 315211 P.R. China*

**e-mail: mouzehuai@nbu.edu.cn*

Received April 11, 2022; revised May 3, 2022; accepted May 4, 2022

Abstract—A series of new N-type functionalized fluorenyl rare-earth metal complexes were synthesized. Treatment of piperidinyl- or hexamethyleneimino-ethylene fluorenyl lithium salts with *in situ* prepared cationic rare-earth metal dialkyl species $[Ln(CH_2SiMe_3)_2(THF)_x][BPh_4]$ afforded readily the corresponding constrained-geometry-complexes $L^1Ln(CH_2SiMe_3)_2$ (L^1 = $FluCH_2CH_2NC_5H_{10}$, Ln = Y (**1-Y**), Lu (**1-Lu**), Sc (**1-Sc**)), $L^2Ln(CH_2SiMe_3)_2$ (L^2 = (2,7-di-*tert*-butyl)$FluCH_2CH_2NC_5H_{10}$, Ln = Y (**2-Y**), Lu (**2-Lu**), Sc (**2-Sc**)) and $L^3Lu(CH_2SiMe_3)_2$ (L^3 = (2,7-di-*tert*-butyl)$FluCH_2CH_2NC_6H_{12}$ (**3-Lu**)) in moderate yields. All these complexes were characterized by NMR spectroscopy, and the solid-state molecular structures of **1-Y** and **2-Sc** were defined with single-crystal X-ray diffraction analysis (CCDC nos. 2157591 (**1-Y**) and 2160297 (**2-Sc**)). The catalytic performance of these complexes towards 2-vinylpyridine polymerization was studied, where these complexes alone could efficiently promote the polymerization of 2-vinylpyridine giving isotactic poly(2-vinylpyridine). The polymerization proceeded in first-order kinetics with respect to both monomer and catalyst concentration.

Keywords: constrained-geometry-configuration, rare-earth metal, stereospecific polymerization, 2-vinylpyridine

DOI: 10.1134/S1070328422330016

INTRODUCTION

In the past decades, organo-rare-earth complexes have experienced great development and exhibited unique performance in various chemical transformations and coordination polymerization [1–3]. Particularly, rare-earth metallocene complexes supported with cyclopentadiene Cp-based ligands (cyclopentadienyl, indenyl and fluorenyl) have occupied a special important place in this area [4–6]. As one of the developed classes of Cp-based ligand, the constrained-geometry-conformation (CGC) ligand featuring a soft or rigid coordinating sidearm could further precisely tune the electronic and steric properties around the central metal [7–10]. To date, various CGC ligands bearing heteroatom-containing (N [11–26], O [27–31], P [32, 33]) as well as N-heterocyclic carbene (NHC) sidearm have been extensively investigated in the organo-rare-earth complexes [34–36]. N-type functionalized Cp ligands have been mostly utilized due to forming strong Ln–N (Ln = rare-earth metal) bonds with the Lewis acidic and hard Ln^{3+} ions via various modes (anionic, neutral, N(sp^2), or N(sp^3)) (Scheme 1) since Bercaw's original work [37], which can stabilize the highly electrophilic rare-earth metal complexes, and promisingly tolerate polar monomers with a heteroatom (N, O, S) in coordination polymerization. The CGC-based rare-earth metal complexes have gained great momentum in the stereoselective (co)polymerization of heteroatom-containing polar styrene in recent years [38–43], while for polymerization of other aromatic polar vinyl monomers, related investigations need to be conducted.

2-Vinylpyridine (2VP) is an important aromatic polar vinyl monomer, and the relative polymers have been widely applied in photochemistry, membrane technology and electrochemistry. During the last decade, the stereospecific polymerization of 2VP with rare-earth non-metallocene complexes has been comprehensively studied [44–55], while Cp-based rare-earth metal complexes were extremely limited [21, 56]. Recently, we reported a series of pyrrolidinyl-ethylene fluorenyl rare-earth metal complexes for stereoselective polymerization of 2VP [57]. In this contribution, we present the synthesis and structures of softer N-type functionalized fluorenyl rare-earth metal complexes. These complexes alone or in the presence of $[Ph_3C][B(C_6F_5)_4]$ exerted varied catalytic performances towards the polymerization of 2VP.

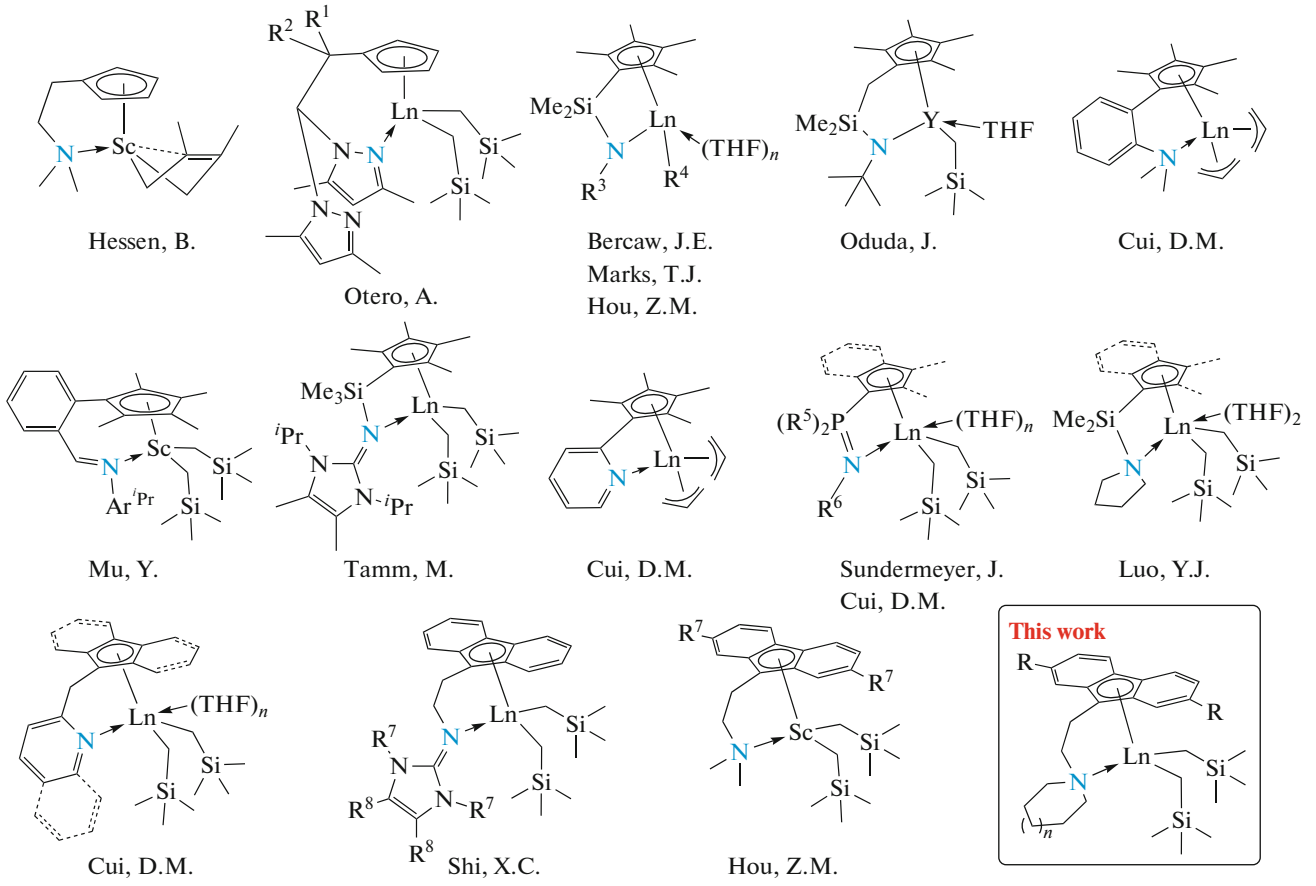

Scheme 1.

EXPERIMENTAL

All reactions were carried out under a dry nitrogen atmosphere using standard Schlenk techniques or in a glove box filled with dry argon. Solvents (THF, hexane and toluene) were dried by distillation over sodium with benzophenone as indicator under an argon atmosphere and were stored over freshly cut sodium in a glove box. $[Ph_3C][B(C_6F_5)_4]$ was purchased from Strem. 2-Vinylpyridine was purchased from Energy Chemical (Shanghai), dried over CaH_2 and distilled prior to use under reduced pressure. *n*-Butyllithium, fluorene, 2,7-di-*tert*-butyl fluorene, $LiCH_2SiMe_3$, 2-piperidinoethyl chloride hydrochloride and 2-(hexamethyleneimino)ethyl chloride hydrochloride were purchased from Energy Chemical (Shanghai) and used as received. Anhydrous YCl_3, $LuCl_3$, $ScCl_3$ and $[Et_3NH][BPh_4]$ were obtained from Prof. Gao at Jilin University. Rare-earth metal tris(alkyl)s was synthesized according to the literature [58]. Thin layer chromatography (TLC) was performed on 0.25 mm Tsingdao silica gel plates (60F-254) and visualized by exposure to UV light (254 nm). Column chromatography was conducted using Tsingdao silica gel (200–300 mesh) under a positive pressure of air. NMR (^1H, ^{13}C) spectra were recorded on a Bruker Ascend 500 spectrometer, 25°C, and referenced internally to residual solvent resonances (C_6D_6: 7.16 ppm for ^1H NMR, 128.06 ppm for ^{13}C NMR; $CDCl_3$: 7.26 ppm for ^1H NMR, 77.16 ppm for ^{13}C NMR; CD_3OD: 3.31 ppm for ^1H NMR, 49.00 ppm for ^{13}C NMR). Molecular weight and molecular weight distribution ($D = M_w/M_n$) were measured by gel permeation chromatography (GPC) analyses carried out at 30°C and a flow rate of 1.0 mL/min with DMF as the eluent on an Agilent PL-GPC50 instrument. High resolution mass spectra were obtained on Aglient 7250&JEOL-JMS-T100LP AccuTOF.

Synthesis of $FluCH_2CH_2NC_5H_{10}$ (HL^1). A *n*-butyllithium (12.5 mL, 1.60 mol/L in hexane) was added dropwise to a suspension of 1-(2-chloroethyl)piperidine hydrochloride (20 mmol, 3.68 g) in THF (50 mL) under stirring at –25°C. Fluorene (21 mmol, 3.49 g) was dissolved in THF (50 mL), and *n*-butyllithium (13.2 mL, 1.60 mol/L in hexane) was added dropwise at –25°C. The two reactions were allowed to stir for 2 h at room temperature. Then the newly generated fluorenyl lithium solution was slowly added to the *in situ* prepared 1-(2-chloroethyl)piperidine solution.

The mixture was stirred for 12 h at 60°C. Then the reaction was quenched with water, and THF was evaporated under reduced pressure. The residue was extracted with ethyl acetate, dried over anhydrous $MgSO_4$, filtered and concentrated. Purification by column chromatography (silica gel 200–300 mesh) was conducted, where excess fluorene was removed first using petroleum ether as eluent, then ethyl acetate was used as eluent to give pure desired ligand as pale-yellow solid (3.22 g, 58%), R_f = 0.21 (EtOAc). ^{1}H NMR (500 MHz; $CDCl_3$; δ, ppm): 7.76 (d., J = 7.5 Hz, 2H, fluorenyl-*H*), 7.53 (d., J = 6.8 Hz, 2H, fluorenyl-*H*), 7.37 (t., J = 7.3 Hz, 2H, fluorenyl-*H*), 7.31 (t.d., J = 7.4, 1.2 Hz, 2H, fluorenyl-*H*), 4.06 (t., J = 5.2 Hz, 1H, fluorenyl-*H*), 2.32 (br., 4H, CH_2), 2.22 (m., 4H, CH_2), 1.56 (m., 4H, CH_2), 1.40 (br., 2H, CH_2). These spectroscopic data are consistent with those reported [59].

Synthesis of $^{t\text{-Bu}}$FluCH$_2$CH$_2$N C$_5$H$_{10}$ (HL^2) was carried out by the same procedure used for HL^1. A reaction 2,7-di-*tert*-butyl fluorene (21 mmol, 5.85 g) with 1-(2-chloroethyl)piperidine hydrochloride (20 mmol, 3.68 g) gave HL^2 as pale-yellow solid (6.31 g, 81%), R_f = 0.24 (EtOAc). ^{1}H NMR (500 MHz; $CDCl_3$; δ, ppm): 7.63 (d., J = 8.0 Hz, 2H, fluorenyl-*H*), 7.54 (s., 2H, fluorenyl-*H*), 7.38 (d.d., J = 8.0, 1.7 Hz, 2H, fluorenyl-*H*), 3.99 (t., J = 5.8 Hz, 1H, fluorenyl-*H*), 2.35 (br., 4H, CH_2), 2.30–2.26 (m., 2H, CH_2), 2.24–2.19 (m., 2H, CH_2), 1.58 (m., 4H, CH_2), 1.42 (m., 2H, CH_2), 1.39 (s., 18H, C(CH_3)$_3$). ^{13}C NMR (125 MHz, $CDCl_3$, δ, ppm): 149.7, 147.4, 138.6, 124.0, 121.4, 119.1, 56.2, 54.8, 46.1, 35.0, 31.8, 30.6, 26.1, 24.6. HRMS (ESI): Exact mass calcd. for [$C_{28}H_{39}N$ + H]$^+$ 390.3155, found 390.3153.

Synthesis of $^{t\text{-Bu}}$FluCH$_2$CH$_2$NC$_6$H$_{12}$ (HL^3) was carried out by the same procedure used for HL^1. A reaction 2,7-di-*tert*-butyl fluorene (21 mmol, 5.85 g) with 2-(hexamethyleneimino)ethyl chloride hydrochloride (20 mmol, 3.96 g) gave HL^3 as pale-yellow solid (6.46 g, 80%), R_f = 0.25 (EtOAc). ^{1}H NMR (500 MHz; $CDCl_3$; δ, ppm): 7.64 (d., J = 8.0 Hz, 2H, fluorenyl-*H*), 7.55 (s., 2H, fluorenyl-*H*), 7.39 (d., J = 8.0 Hz, 2H, fluorenyl-*H*), 4.02 (t., J = 5.9 Hz, 1H, fluorenyl-*H*), 2.65 (m., 4H, CH_2), 2.49 (m., 2H, CH_2), 2.18 (d.d., J = 14.4, 6.9 Hz, 2H, CH_2), 1.64 (br., 4H, CH_2), 1.58 (br., 4H, CH_2), 1.40 (s., 18H, C(CH_3)$_3$]. ^{13}C NMR (125 MHz; $CDCl_3$; δ, ppm): 149.7, 147.6, 138.6, 124.0, 121.4, 119.1, 55.6, 54.8, 45.9, 35.0, 31.8, 31.3, 28.2, 27.1. HRMS (ESI): Exact mass calcd. for [$C_{29}H_{41}N$ + H]$^+$ 404.3312, found 404.3307.

Synthesis of L^{1}Li(THF)$_2$. To a THF (20 mL) solution of HL^1 (5.0 mmol, 1.39 g) was added dropwise *n*-butyllithium (3.2 mL, 1.60 mol/L in hexane) at –25°C, the reaction solution was stirred for 4 h at room temperature. The volatile was removed under reduced pressure, and the residue was washed with hexane to afford the title lithium salt as yellow solid (2.08 g, 97%). ^{1}H NMR (500 MHz; C_6D_6; δ, ppm): 8.42 (d., J = 7.8 Hz, 2H, fluorenyl-*H*), 7.71 (d., J = 8.2 Hz, 2H, fluorenyl-*H*), 7.52 (m., 2H, fluorenyl-*H*), 3.41 (t., J = 6.1 Hz, 2H, CH_2), 2.86 (br., 8H, *THF*), 2.65 (t., J = 6.1 Hz, 2H, CH_2), 2.17 (br., 4H, CH_2), 1.20 (br., 8H, *THF*), 0.96 (br., 6H, CH_2).

Synthesis of L^{2}Li(THF)$_2$. To a THF solution of HL^2 (5.0 mmol, 1.95 g) was added dropwise *n*-butyllithium (3.2 mL, 1.60 mol/L in hexane) at –25°C, the reaction solution was stirred for 4 h at room temperature. The volatile was removed under reduced pressure, and the residue was washed with hexane to afford the title lithium salt as yellow solid (2.54 g, 94%). ^{1}H NMR (500 MHz; C_6D_6; δ, ppm): 8.31 (d., J = 8.3 Hz, 2H, fluorenyl-*H*), 7.71 (s., 2H, fluorenyl-*H*), 7.14 (d.d., J = 8.3, 1.7 Hz, 2H, fluorenyl-*H*), 3.50 (t., J = 6.1 Hz, 2H, CH_2), 2.91 (br., 8H, *THF*), 2.72 (t., J = 6.1 Hz, 2H, CH_2), 2.20 (br., 4H, CH_2), 1.62 (s., 18H, C(CH_3)$_3$), 1.23 (br., 8H, *THF*), 0.99 (br., 6H, CH_2).

Synthesis of L^{3}Li(THF)$_{3.5}$. To a THF solution of HL^3 (5.0 mmol, 2.02 g) was added dropwise *n*-butyllithium (3.2 mL, 1.60 mol/L in hexane) at –25°C, the reaction solution was stirred for 4 h at room temperature. The volatile was removed under reduced pressure, and the residue was washed with hexane to afford the title lithium salt as yellow solid (3.50 g, 98%). ^{1}H NMR (500 MHz; C_6D_6; δ, ppm): 8.33 (d., J = 8.3 Hz, 2H, fluorenyl-*H*), 7.73 (s., 2H, fluorenyl-*H*), 7.14 (m., 2H, fluorenyl-*H*), 3.47 (t., J = 6.0 Hz, 2H, CH_2), 3.34 (br., 14H, *THF*), 2.88 (t., J = 6.0 Hz, 2H, CH_2), 2.35 (br., 4H, CH_2), 1.62 (s., 18H, C(CH_3)$_3$), 1.29 (br., 14H, *THF*), 1.15 (br., 8H, CH_2).

Synthesis of 1-Y. In the glovebox, Y(CH_2SiMe$_3$)$_3$-(THF)$_2$ (0.5 mmol, 0.25 g) and [Et_3NH][BPh_4] (0.5 mmol, 0.21 g) were mixed in THF (5 mL) at room temperature and stirred for several minutes, then a THF solution of L^{1}Li(THF)$_2$ (0.5 mmol, 0.22 g) was added slowly into the mixture. The reaction mixture was stirred for 2 h. Volatiles were removed under reduced pressure, and the residue was extracted with 10 mL of toluene–hexane mixed solution (v/v = 1/1). The suspension was filtered, and the filtrate was concentrated and crystalized at –25°C to give the title complex as yellow solid (0.16 g, 61%). Single crystals suitable for X-ray diffraction analysis were obtained with recrystallization from saturated toluene–hexane mixed solution at –25°C after a few days. ^{1}H NMR (500 MHz; C_6D_6; δ, ppm): 8.21 (d., J = 8.3 Hz, 2H, fluorenyl-*H*), 7.31–7.30 (m., 4H, fluorenyl-*H*), 7.20–7.16 (m., 2H, fluorenyl-*H*), 2.97 (br., 2H, CH_2), 2.79 (t., J = 6.1 Hz, 2H, CH_2), 2.48 (t., J = 6.1 Hz, 2H, CH_2), 1.51 (br., 2H, CH_2), 1.22 (br., 5H, CH_2), 0.75 (br., 1H, CH_2), 0.18 (s., 18H, Si(CH_3)$_3$), –1.49

(d., J_{Y-H} = 26.9 Hz, 4H, Y-CH_2). ^{13}C NMR (125 MHz; C_6D_6; δ, ppm): 131.6, 126.3, 124.3, 119.1, 118.0, 117.6, 93.8, 59.7, 53.1, 39.8 (d., J_{Y-C} = 43.6 Hz), 23.5, 23.1, 20.8, 4.3.

For $C_{28}H_{44}NSi_2Y$

Anal. calcd., %	C, 62.31	H, 8.22	N, 2.60
Found, %	C, 62.23	H, 8.26	N, 2.65

Synthesis of 1-Lu. Following the similar procedure, using $Lu(CH_2SiMe_3)_3(THF)_2$ (0.5 mmol, 0.29 g) and $L^1Li(THF)_2$ (0.5 mmol, 0.22 g), gave complex **1-Lu** as yellow solids (0.18 g, 56%). ^{1}H NMR (500 MHz; C_6D_6; δ, ppm): 8.22 (d., J = 8.3 Hz, 2H, fluorenyl-*H*), 7.33–7.27 (m., 4H, fluorenyl-*H*), 7.21–7.18 (m., 2H, fluorenyl-*H*), 2.94 (br., 2H, CH_2), 2.77 (t., J = 6.1 Hz, 2H, CH_2), 2.52 (t., J = 6.1 Hz, 2H, CH_2), 1.72 (br., 2H, CH_2), 1.18 (br., 5H, CH_2), 0.81 (br., 1H, CH_2), 0.17 (s., 18H, Si(CH_3)$_3$), −1.68 and −1.86 (AB, $^2J_{H-H}$ = 9.4 Hz, 4H, Lu–CH_2). ^{13}C NMR (125 MHz, C_6D_6; δ, ppm): 131.7, 126.2, 124.6, 119.0, 118.2, 117.3, 92.1, 58.2, 52.5, 44.1, 23.1, 22.3, 20.5, 4.4.

For $C_{28}H_{44}LuNSi_2$

Anal. calcd., %	C, 53.74	H, 7.09	N, 2.24
Found, %	C, 53.76	H, 7.12	N, 2.30

Synthesis of 1-Sc. Following the similar procedure, using $Sc(CH_2SiMe_3)_3(THF)_2$ (0.5 mmol, 0.23 g) and $L^1Li(THF)_2$ (0.5 mmol, 0.22 g), gave complex **1-Sc** as yellow solids (0.12 g, 50%). ^{1}H NMR (500 MHz; C_6D_6; δ, ppm): 8.24 (d., J = 8.3 Hz, 2H, fluorenyl-*H*), 7.32–7.26 (m., 4H, fluorenyl-*H*), 7.21–7.18 (m., 2H, fluorenyl-*H*), 2.98 (m., 2H, CH_2), 2.73 (t., J = 6.0 Hz, 2H, CH_2), 2.64 (t., J = 6.0 Hz, 2H, CH_2), 2.11 (br., 2H, CH_2), 1.18–1.12 (m., 4H, CH_2), 1.10–0.97 (m., 2H, CH_2), 0.15 (s., 18H, Si(CH_3)$_3$), −1.11 (s., 4H, Sc–CH_2). ^{13}C NMR (125 MHz; C_6D_6; δ, ppm): 130.9, 128.1, 125.9, 124.9, 119.8, 119.6, 119.0, 95.3, 55.9, 52.4, 46.5, 23.2, 20.9, 20.7, 4.0.

For $C_{28}H_{44}NScSi_2$

Anal. calcd., %	C, 67.83	H, 8.95	N, 2.83
Found, %	C, 67.89	H, 8.86	N, 2.75

Synthesis of 2-Y. Following the similar procedure, using $Y(CH_2SiMe_3)_3(THF)_2$ (0.5 mmol, 0.23 g) and $L^2Li(THF)_2$ (0.5 mmol, 0.27 g), gave **2-Y** as yellow solids (0.21 g, 63%). ^{1}H NMR (500 MHz; C_6D_6; δ, ppm): 8.22 (d., J = 8.7 Hz, 2H, fluorenyl-*H*), 7.46 (s., 2H, fluorenyl-*H*), 7.30 (d.d., J = 8.7, 1.7 Hz, 2H, fluorenyl-*H*), 3.17 (d., J = 11.0 Hz, 2H, CH_2), 2.94 (t., J = 6.0 Hz, 2H, CH_2), 2.54 (t., J = 5.5 Hz, 2H, CH_2), 1.47 (s., 18H, C(CH_3)$_3$), 1.43–1.34 (m., 4H, CH_2), 1.26–1.20 (m., 3H, CH_2), 0.76–0.67 (m., 1H, CH_2), 0.20 (s., 18H, Si(CH_3)$_3$), −1.38 and −1.75 (AB, $^2J_{H-H}$ = 11.0 Hz, 4H, Y–CH_2). ^{13}C NMR (125 MHz; C_6D_6; δ, ppm): 148.4, 132.1, 123.8, 118.5, 115.5, 113.0, 93.9, 60.5, 53.7, 39.1 (d., J_{Y-C} = 43.5 Hz), 35.3, 31.8, 24.2, 23.1, 20.8, 4.5.

For $C_{36}H_{60}NSi_2Y$

Anal. calcd., %	C, 66.32	H, 9.28	N, 2.15
Found, %	C, 66.28	H, 9.26	N, 2.21

Synthesis of 2-Lu. Following the similar procedure, using $Lu(CH_2SiMe_3)_3(THF)_2$ (0.5 mmol, 0.29 g) and $L^2Li(THF)_2$ (0.5 mmol, 0.27 g), gave complex **2-Lu** as yellow solids (0.25 g, 68%). ^{1}H NMR (500 MHz; C_6D_6; δ, ppm): 8.22 (d., J = 8.8 Hz, 2H, fluorenyl-*H*), 7.46 (s., 2H, fluorenyl-*H*), 7.31 (d.d., J = 8.8, 1.7 Hz, 2H, fluorenyl-*H*), 3.15 (d., J = 12.2 Hz, 2H, CH_2), 2.92 (t., J = 6.0 Hz, 2H, CH_2), 2.56 (t., J = 5.4 Hz, 2H, CH_2), 1.64 (t., J = 10.8 Hz, 2H, CH_2), 1.47 (s., 18H, C(CH_3)$_3$), 1.42–1.35 (m., 2H, CH_2), 1.21–1.15 (m., 3H, CH_2), 0.80–0.71 (m., 1H, CH_2), 0.20 (s., 18H, Si(CH_3)$_3$), −1.65 and −2.01(AB, $^2J_{H-H}$ = 11.2 Hz, 4H, Lu–CH_2). ^{13}C NMR (125 MHz; C_6D_6; δ, ppm): 148.3, 132.1, 124.1, 118.4, 115.1, 113.1, 92.1, 59.3, 53.2, 43.8, 35.3, 31.8, 23.1, 20.5, 4.7.

For $C_{36}H_{60}LuNSi_2$

Anal. calcd., %	C, 58.59	H, 8.19	N, 1.90
Found, %	C, 58.62	H, 8.26	N, 1.83

Synthesis of 2-Sc. Following the similar procedure, using $Sc(CH_2SiMe_3)_3(THF)_2$ (0.5 mmol, 0.23 g) and $L^2Li(THF)_2$ (0.5 mmol, 0.27 g), gave complex **2-Sc** as yellow solids (0.16 g, 53%). Crystals suitable for X-ray diffraction analysis were grown from saturated hexane solution at −25°C. ^{1}H NMR (500 MHz; C_6D_6; δ, ppm): 8.23 (d., J = 8.8 Hz, 2H, fluorenyl-*H*), 7.46 (s., 2H, fluorenyl-*H*), 7.32 (d.d., J = 8.8, 1.6 Hz, 2H, fluorenyl-*H*), 3.17 (m, 2H, CH_2), 2.89 (t, J = 6.1 Hz, 2H, CH_2), 2.72 (t., J = 5.8 Hz, 2H, CH_2), 2.11 (br., 2H, CH_2), 1.46 (s., 18H, C(CH_3)$_3$), 1.26 (m., 2H, CH_2), 1.20 (m., 2H, CH_2), 1.11 (m., 1H, CH_2), 0.99 (m., 1H, CH_2), 0.18 (s., 18H, Si(CH_3)$_3$), −1.03 and −1.29 (AB, $^2J_{H-H}$ = 10.9 Hz, 4H, Sc–CH_2). ^{13}C NMR (125 MHz; C_6D_6; δ, ppm): 148.01, 131.47, 124.56, 119.32, 116.85, 114.35, 95.48, 56.76, 52.94, 45.81, 35.31, 31.69, 23.30, 21.35, 20.86, 4.22.

For $C_{36}H_{60}NScSi_2$

Anal. calcd., %	C, 71.12	H, 9.95	N, 2.30
Found, %	C, 71.15	H, 9.91	N, 2.33

Synthesis of 3-Lu. Following the similar procedure, using $Lu(CH_2SiMe_3)_3(THF)_2$ (0.5 mmol, 0.29 g) and $L^3Li(THF)_{3.5}$ (0.5 mmol, 0.38 g), gave complex **3-Lu** as yellow solids (0.19 g, 50%). ^1H NMR (500 MHz; C_6D_6; δ, ppm): 8.20 (d., J = 8.7 Hz, 2H, fluorenyl-*H*), 7.49 (s., 2H, fluorenyl-*H*), 7.31 (d.d., J = 8.7, 1.6 Hz, 2H, fluorenyl-*H*), 2.90 (t., J = 6.1 Hz, 2H, CH_2), 2.84 (br., 2H, CH_2), 2.76 (t., J = 6.1 Hz, 2H, CH_2), 2.60 (br., 2H, CH_2), 1.49 (s., 18H, C(CH_3)$_3$), 1.28 (br., 4H, CH_2), 1.11 (br., 4H, CH_2), 0.19 (s., 18H, Si(CH_3)$_3$), −1.69 and −1.90 (AB, $^2J_{H-H}$ = 11.3 Hz, 2H, Lu−CH_2). ^{13}C NMR (125 MHz; C_6D_6; δ, ppm): 148.3, 132.6, 124.0, 118.5, 115.1, 113.3, 92.5, 56.2, 52.9, 41.9, 35.3, 31.8, 27.8, 23.2, 21.4, 4.7.

For $C_{37}H_{62}LuNSi_2$			
Anal. calcd., %	C, 59.09	H, 8.31	N, 1.86
Found, %	C, 59.05	H, 8.36	N, 1.89

General procedures for 2VP polymerization. *Single component catalysis.* Polymerization were conducted in 20 mL of oven-dried vial inside glovebox under ambient temperature (~28°C). The dialkyl complex (10 μmol) was dissolved in 1.0 mL of toluene, then 200 equiv. of 2VP with 0.8 mL of toluene was added into the mixture in one portion. After a required time, the polymerization was quenched with a few drops of methanol, and the resulting polymer was precipitated from 50 mL of petroleum ether or hexane, then dried in vacuum oven at 50°C to a constant weight.

Binary catalysis. Polymerization were conducted in 20 mL of oven-dried vial inside glovebox under ambient temperature (~28°C). $[Ph_3C][B(C_6F_5)_4]$ (10 μmol, 1.0 eq.) and dialkyl complex (10 μmol, 1.0 eq.) were dissolved in 0.9 mL of solvent respectively, and the borate solution was added dropwise into the dialkyl complex solution under stirring, then 200 equivalents of 2VP was added into the mixture in one portion. After a required time, the polymerization was quenched with a few drops of methanol, and the resulting polymer was precipitated from 50 mL of petroleum ether or hexane, then dried in vacuum oven at 50°C to a constant weight.

Kinetic experiment. 0.21 g (2.0 mmol) of 2VP was rapidly added into a toluene solution (3.8 mL) of catalyst (20 μmol) under stirring ($[2VP]_o$ = 0.5 M). After certain time interval, 0.2 mL aliquots were taken from the polymerization solution and quickly quenched into 0.4 mL of $CDCl_3$ containing few ethanol. The quenched aliquots were analysed by ^1H NMR spectroscopy to determine the monomer conversions.

Single crystal X-ray diffraction analysis. Suitable single crystals of complexes were sealed in polybutene for determining the single-crystal structure. Data were collected on a Bruker D8 QUEST diffractometer using Cu (60 W, diamond, μK_α = 12.894 mm^{-1}) micro-focus X-ray sources. The structures were solved and refined using the SHELXL-97 program, and refined by full-matrix least-squares procedures based on $|F|^2$. All the non-hydrogen atoms were refined anisotropically. Molecular structures were generated using the ORTEP program.

The supplementary crystallographic data were deposited with the Cambridge Crystallographic Data Centre (CCDC nos. 2157591 **(1-Y)** and 2160297 (**2-Sc**); www.ccdc.cam.ac.uk/data_request/cif, or by emailing data_request@ccdc.cam.ac.uk).

RESULTS AND DISCUSSION

The piperidinyl-ethylene fluorene ligands $FluCH_2CH_2NC_5H_{10}$ (HL^1) and (2,7-di-*tert*-butyl)$FluCH_2CH_2NC_5H_{10}$ (HL^2) and hexamethyleneimino-ethylene ditertbutyl fluorene ligand (2,7-di-*tert*-butyl)$FluCH_2CH_2NC_6H_{12}$ (HL^3) were synthesized by the lithiation of fluorene or 2,7-di-tert-butyl fluorene with *n*-butyllithium followed by addition of the lithium salt into a THF solution of 2-piperidinoethyl chloride or 2-(hexamethyleneimino)ethyl chloride which were *in situ* generated with the reaction between *n*-butyllithium and 2-piperidinoethyl chloride hydrochloride or 2-(hexamethyleneimino)ethyl chloride hydrochloride (Scheme 2). In the ^1H NMR spectra, the methenyl proton (−C*H*−) gave a triplet at 4.06 ppm (J = 5.2 Hz, HL^1, Fig. S1), 3.99 ppm (J = 5.8 Hz, HL^2, Fig. S2) and 4.02 ppm (J = 5.9 Hz, HL^3, Fig. S4) in $CDCl_3$, respectively. The three ligands could be readily converted to lithium salts in excellent yields (97% for HL^1, 94% for HL^2, and 98% for HL^3), and the ^1H NMR spectra in C_6D_6 (Figs. S6–S8) showed the resulting lithium salts were coordinated with 2 (for L^1 and L^2, Figs. S6, S7) or 3.5 (for L^3, Fig. S8) THF molecules. Treatment of ligand lithium salts with *in situ* prepared rare-earth metal alkyl ion-pair complexes $[Ln(CH_2SiMe_3)_2(THF)_x][BPh_4]$ (Ln = Y, Lu, Sc), reported by Okuda in THF at room temperature afforded desired rare-earth metal dialkyl complexes $L^1Ln(CH_2SiMe_3)_2$ (Ln = Y (**1-Y**), Lu (**1-Lu**), Sc (**1-Sc**)), $L^2Ln(CH_2SiMe_3)_2$ (Ln = Y (**2-Y**), Lu (**2-Lu**), Sc (**2-Sc**)) and $L^3Lu(CH_2SiMe_3)_2$ (**3-Lu**) as yellow solids in moderate yields (50–68%) (Scheme 3). These complexes showed well resolved ^1H and ^{13}C NMR spectra in C_6D_6 (see supporting information). The ^1H NMR spectra of these six complexes clearly showed the absence of methenyl proton on fluorenyl ring, and confirmed the formation of dialkyl complexes based on the integral area ratios of ligand moieties and silylalkyl segments. Besides, no any signals from THF were observed, indicating that THF-free complexes were formed. The methylene protons of the two silylalkyls (Ln−CH_2SiMe$_3$) gave obviously different signals in this series rare-earth complexes.

The methylene protons of $-CH_2SiMe_3$ in complex **1-Y** showed a doublet at −1.49 ppm with a J_{Y-H} of 26.9 Hz, and displayed a singlet at −1.11 ppm in complex **1-Sc**, suggesting the two silylalkyls are equivalent in solution. In contrast, the two silylalkyl groups in lutetium complexes (**1-Lu**, **2-Lu** and **3-Lu**), yttrium complex **2-Y** and scandium complex **2-Sc** exhibited AB spin at −1.68, −1.86 ppm ($^2J_{H-H}$ = 9.4 Hz, for **1-Lu**), −1.38, −1.75 ppm ($^2J_{H-H}$ = 11.0 Hz, for **2-Y**), −1.65, −2.01 ppm ($^2J_{H-H}$ = 11.2 Hz, for **2-Lu**), −1.03, −1.29 ppm ($^2J_{H-H}$ = 10.9 Hz, for **2-Sc**) and −1.69, −1.90 ppm ($^2J_{H-H}$ = 11.3 Hz, for **3-Lu**), respectively, indicating that the methylene protons are diastereotopic and the rotation of the $-CH_2SiMe_3$ group was restricted to some extent on the NMR time scale due to steric hindrance. The molecular structures of complexes **1-Y** and **2-Sc** were confirmed by single crystal X-ray diffraction as depicted in Fig. 1, although the raw crystallographic data of **1-Y** was not good enough. The CGC ligand coordinated to the metal center in a typical η^5/κ^1 fashion via the Cp ring and the sidearm N atom, and the selected bong lengths and angles were listed in Table 1. No coordinated THF molecule was observed in crystal structures of both complexes as ^{1}H NMR spectra showed. Y(1)–N(1) bond length of 2.463(6) Å and bite angle $Cp_{cent}Y(1)N(1)$ (cent: centroid) of 97.95° are both similar with those in the analogous pyrrolidinyl-functionalized fluorenyl yttrium complex reported recently, despite the bond lengths of Y(1)–C(Cp) fall in a wider range from 2.609(7) to 2.774(8) Å with a slightly longer $Y(1)-Cp_{cent}$ distance of 2.411 Å [57]. In complex **2-Sc**, the bond lengths of Sc(1)–C(Cp) are in the range of 2.4727(17) to 2.6096(17) Å with a $Sc(1)-C(Cp)_{av}$ (av: average) distance of 2.5601 Å and $Sc(1)-Cp_{cent}$ distance of 2.253 Å, both are slightly longer than those in the dimethylamino-functionalized fluorenyl scandium complex because of the bulkier piperidinyl group [22].

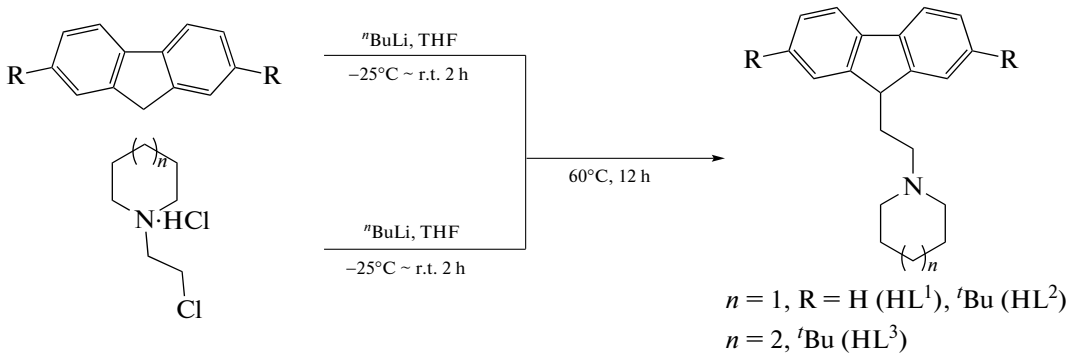

Scheme 2.

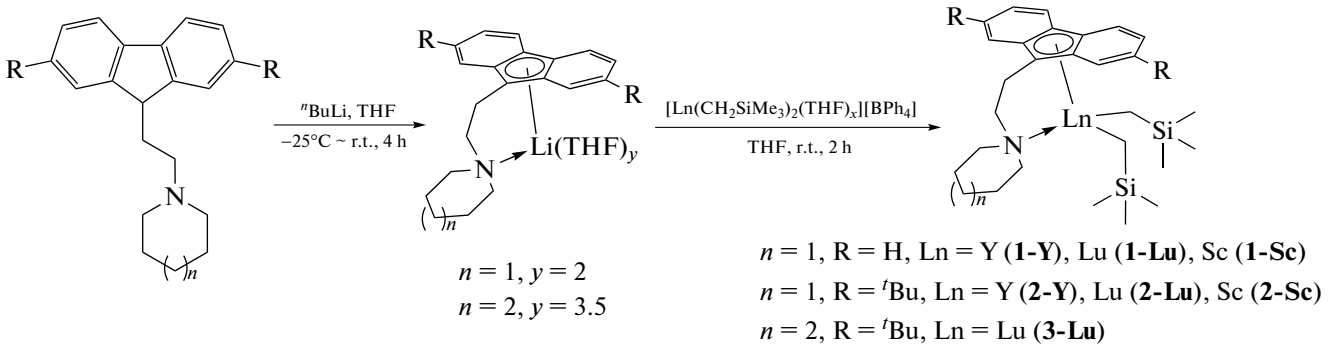

Scheme 3.

The catalytic performances of these new CGC-type rare-earth metal diakyl complexes towards 2VP polymerization were investigated, and the results are summarized in Table 2. Yttrium and lutetium complexes efficiently promoted the 2VP polymerization in toluene at ambient temperature (~28°C), affording almost quantitative polymer yields of 200 equivalents of monomer within 10 min (Table 2, entries 1–2 and 4–6), while the less active scandium complexes only achieved moderate yields (**1-Sc**: 55% yield, **2-Sc**: 48% yield) in 60 min (Table 2, entries 3 and 6). The molecular weights obtained from GPC data are close to the theoretical values based on one polymer chain growing per metal center, and molecular weight distributions (*D*) stay between 1.86 and 2.42, suggesting that this series of soft N-type CGC rare-earth complexes exerted better controllability over the recent reports [21, 57]. ^{13}C NMR spectra showed that the resultant

Table 1. Selected bond lengths (Å) and angles (deg) for complexes **1-Y** and **2-Sc**

Compound	**1-Y**	**2-Sc**
Bond lengths	*d*, Å	
Ln(1)–N(1)	2.463(6)	2.3688(15)
Ln(1)–C(1)	2.697(7)	2.5494(17)
Ln(1)–C(6)	2.774(8)	2.6096(17)
Ln(1)–C(7)	2.742(8)	2.6096(16)
Ln(1)–C(12)	2.674(7)	2.5594(17)
Ln(1)–C(13)	2.609(7)	2.4727(17)
Ln(1)–C(Cp)$_{av}$	2.6992	2.5601
Ln(1)–C(21)	2.364(7)	2.212(2)
Ln(1)–C(25)	2.380(6)	2.2059(19)
Ln(1)–Cp$_{cent}$	2.411	2.253
Bond angles	ω, deg	
N(1)Ln(1)C(13)	69.9(2)	73.39(6)
N(1)Ln(1)C(21)	118.3(2)	102.25(8)
N(1)Ln(1)C(25)	110.9(2)	108.42(6)
C(21)Ln(1)C(25)	105.3(2)	109.86(9)
N(1)Ln(1)Cp$_{cent}$	97.95	102.78

P2VP are isotactic-enriched with mm values ranging from 0.58 to 0.90, where the isoselectivity trend followed the order of Lu > Sc > Y, being consistent with previous work [57]. Comparing lutetium complexes in this series, complex **2-Lu** bearing tertbutyl group on fluorenyl exerted higher isoselectivity than that of complex **1-Lu** (Table 2, entry 5 vs 2), and complex **3-Lu** bearing seven-membered imino sidearm did not exhibit better stereoselectivity than complex **2-Lu** did (Table 2, entry 7 vs 5). When the polymerization was performed at 0°C, complex **2-Lu** could afford 90% yield within 30 min, while the stereoselectivity was substantially enhanced with mm value up to 0.95 (Table 1, entry 8). Further lowering polymerization temperature to –20°C did not afford obvious improvement in isoselectivity (Table 2, entry 9).

In our recent work, first-order kinetics on 2VP concentration have been established for the 2VP polymerization promoted by analogous pyrrolidinyl-functionalized fluorenyl rare-earth metal complexes

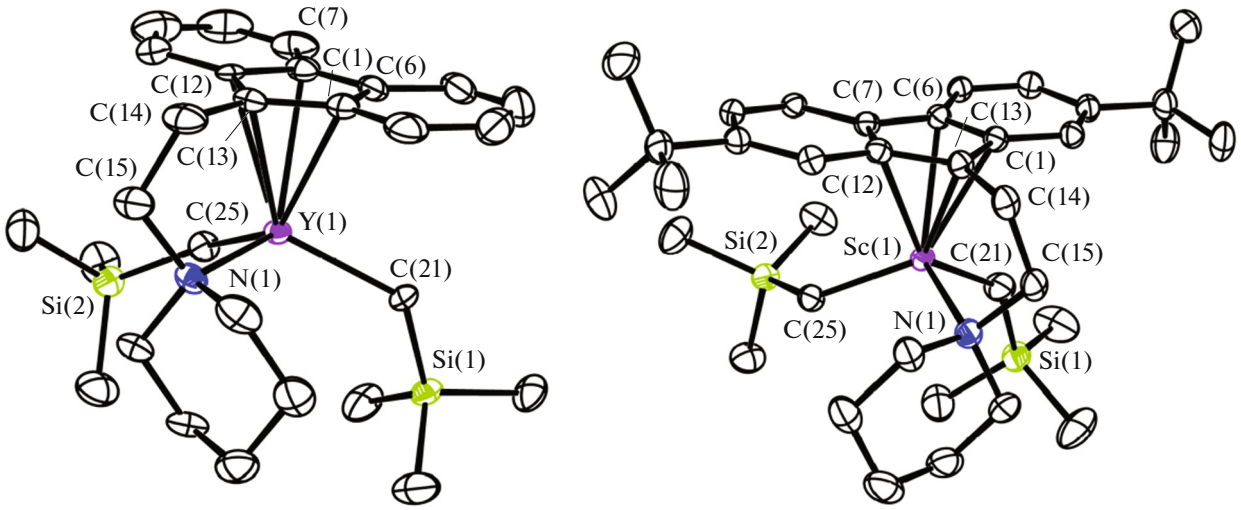

Fig. 1. X-ray crystal structures of complexes **1-Y** and **2-Sc**. Thermal ellipsoids are drawn at 30% probability level and hydrogen atoms have been omitted for clarity.

Table 2. 2-Vinylpyridine polymerization under various conditions*

Entry	Cat.	T, °C	Time, min	Yield, %	$M_{n,exp}$, kg/mol	$Đ$	mm
1	**1-Y**	28	10	98	27.8	1.86	0.58
2	**1-Lu**	28	10	100	24.1	1.95	0.74
3	**1-Sc**	28	60	55	9.9	2.42	0.68
4	**2-Y**	28	10	98	31.3	2.05	0.70
5	**2-Lu**	28	10	100	21.4	2.17	0.90
6	**2-Sc**	28	60	48	9.1	2.29	0.79
7	**3-Lu**	28	10	100	22.6	2.31	0.90
8	**2-Lu**	0	30	90	16.5	2.06	0.95
9	**2-Lu**	−20	60	100	19.9	2.12	0.96

* Conditions: solvent: toluene, [2VP] = 1.0 M, [2VP]/Cat. = 200/1, Cat.: 10 μmol; yield determined by gravimetry. The molecular weight ($M_{n,exp}$) and distribution ($Đ$) were determined by gel permeation chromatography (GPC) in DFM; mm is an isotactic triad and determined with the integral of aromatic quaternary carbon in the ^{13}C NMR spectrum (CD_3OD, 125 MHz).

[57], but the kinetics on catalyst concentration is still unknown. Taking piperidinyl-functionalized complex **2-Lu** as the catalyst, kinetic studies of 2VP polymerization were conducted in toluene at 28°C, where monomer concentration $[2VP]_o$ was fixed at 0.5 M in view of its high activity, and the monomer to catalyst ratio $[2VP]_o/[\mathbf{2\text{-}Lu}]_o$ varied from 100 to 400. The plots of $\ln([M]_o/[M]_t)$ versus time were fitted linearly in all cases (Fig. 2), showing a first-order kinetics dependence on 2VP concentration. Furthermore, a plot of $\ln(K_{app})$ (K_{app}: apparent rate constant) versus ln[Lu] was fitted to a straight line with a slope of 1.060 (R^2 = 0.997, Fig. 3). Thus, the kinetic order with respect to [Lu] also complies with first-order, and the polymerization rate law could be depicted as $-d[2VP]/dt = k_p[2VP][Lu]$, where k_p is the propagation rate constant. These results are similar with the monometallic mechanism established for the 2VP polymerization mediated by bis(phenolate)yttrium alkyl complexes [47, 61].

Taking complexes **2-Lu** and **2-Sc** for examples, catalytic properties of binary system **2-Ln**/$[Ph_3C][B(C_6F_5)_4]$ were studied, and the polymerization data were collected in Table 3. Upon the activation of $[Ph_3C][B(C_6F_5)_4]$, the **2-Lu** based cationic system revealed lower activity and isoselectivity than the corresponding neutral one, needing 90 min to achieve quantitative yield and affording P2VP with mm value of 0.77 (Table 3, entry 1). The **2-Sc** based cationic system exerted comparable activity to the neutral one, but

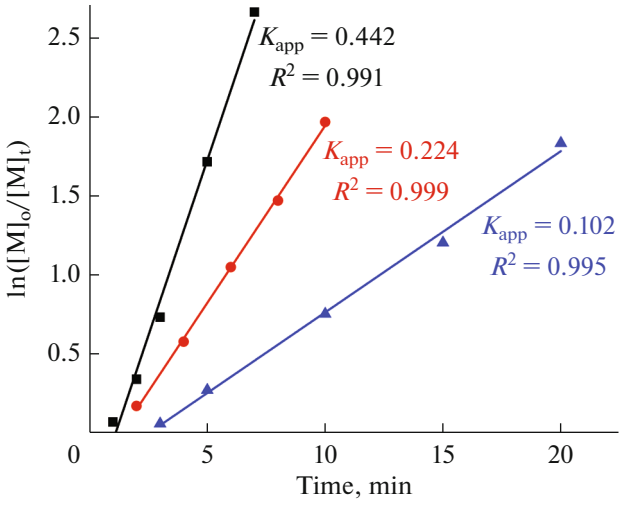

Fig. 2. Plots of $\ln([M]_o/[M]_t)$ versus time for the 2VP polymerization catalyzed by **2-Lu** with varied catalyst concentrations: $[\mathbf{2\text{-}Lu}]_o$ = 1.25 mM (blue, $[2VP]_o/[\mathbf{2\text{-}Lu}]_o$ = 400), 2.50 mM (red, $[2VP]_o/[\mathbf{2\text{-}Lu}]_o$ = 200), and 5.00 mM (black, ($[2VP]_o/[\mathbf{2\text{-}Lu}]_o$ = 100). Polymerization conditions: 28°C, toluene, $[2VP]_o$ = 0.50 M.

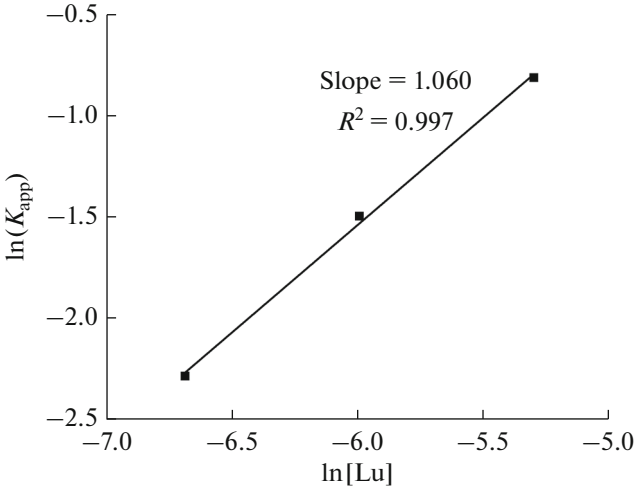

Fig. 3. Plots of $\ln(K_{app})$ versus ln[Lu] for the 2VP polymerization catalyzed by **2-Lu**. Reaction conditions: 28°C, toluene, $[2VP]_o$ = 0.50 M.

Table 3. 2-Vinylpyridine polymerization in the presence of $[Ph_3C][B(C_6F_5)_4]$*

Entry	Cat.	Solvent	T, °C	Time, min	Yield, %	$M_{n,exp}$, kg/mol	$Đ$	mm	*rr*
1	**2-Lu**	Toluene	28	90	100	23.5	1.89	0.77	0.10
2	**2-Sc**	Toluene	28	90	91	22.9	2.20	0.19	0.52
3	**2-Sc**	PhCl	28	90	98	20.2	2.13	0.16	0.55
4	**2-Sc**	Toluene	0	240	43	9.0	2.27	0.15	0.59
5	**2-Sc**	PhCl	0	240	61	11.3	2.58	0.14	0.62

* Conditions: [2VP] = 1.0 M, [2VP]/Cat. = 200/1, Cat.: 10 μmol, $[Ph_3C][B(C_6F_5)_4]$: 10 μmol; yield determined by gravimetry; the molecular weight ($M_{n,exp}$) and distribution ($Đ$) were determined by gel permeation chromatography (GPC) in DMF; mm is an isotactic triad, and *rr* is a syndiotactic triad determined with the integral of aromatic quaternary carbon in the ^{13}C NMR spectrum (CD_3OD, 125 MHz).

gave opposite stereoselectivity, affording syndio-enriched P2VP with *rr* value of 0.52 (Table 3, entry 2). Using chlorobenzene (PhCl) as polymerization solvent, the activity (98% yield) and syndioselectivity (*rr*: 0.55) were both slightly increased (Table 3, entry 3). Reduction of polymerization temperature to 0°C enhanced *rr* values to 0.59 and 0.62, but only gave moderate yields extending time to 240 min (Table 3, entries 4 and 5).

Thus, the present work has documented that soft six-membered and seven-membered imino functionalized fluorenyl ligands could stabilize rare-earth metal via η^5/κ^1 coordination mode and form THF-free CGC-based dialkyl complexes. These complexes efficiently promoted 2VP stereospecific polymerization affording moderate to highly isotactic P2VP without any activator. The kinetic experiments revealed the 2VP polymerization followed first-order in both monomer and catalyst concentration. In the presence of $[Ph_3C][B(C_6F_5)_4]$, the scandium complex exhibited opposite stereoselectivity affording syndio-rich P2VP.

FUNDING

The authors acknowledge financial support from the National Natural Science Foundation of China (no. 21805143), the Natural Science Foundation of Zhejiang Province (no. LY21B040002), and the K.C. Wong Magna Fund from Ningbo University.

CONFLICT OF INTEREST

The authors declare that they have no conflicts of interest.

SUPPLEMENTARY INFORMATION

The online version contains supplementary material available at https://doi.org/10.1134/S1070328422330016 and are accessible for authorized users.

REFERENCES

1. Nishiura, M. and Hou, Z., *Nat. Chem.*, 2010, vol. 2, p. 257.
2. Huang, J., Liu, Z., Cui, D., et al., *ChemCatChem*, 2018, vol. 10, p. 42.
3. Lyubov, D.M., Tolpygin, A.O., and Trifonov, A.A., *Coord. Chem. Rev.*, 2019, vol. 392, p. 83.
4. Nishiura, M. and Hou, Z., *Bull. Chem. Soc. Jpn.*, 2010, vol. 83, p. 595.
5. Arndt, S. and Okuda, J., *Chem. Rev.*, 2002, vol. 102, p. 1953.
6. Luo, Y., Chen, F., and Chen, J., *Z. Anorg. Allg. Chem.*, 2018, vol. 644, p. 405.
7. Arndt, S., Beckerle, K., Hultzsch, K.C., et al., *J. Mol. Catal., A.*, 2002, vol. 190, p. 215.
8. Tian, S., Arredondo, V.M., Stern, C.L., et al., *Organometallics*, 1999, vol. 18, p. 2568.
9. Kirillov, E., Toupet, L., Lehmann, C.W., et al., *Organometallics*, 2003, vol. 22, p. 4467.
10. Mu, Y., Piers, W.E., MacDonald, M.-A., et al., *Can. J. Chem.*, 1995, vol. 73, p. 2233.
11. Weger, M., Pahl, P., Schmidt, F., et al., *Macromolecules*, 2019, vol. 52, p. 7073.
12. Zhang, W.-X., Nishiura, M., and Hou, Z., *J. Am. Chem. Soc.*, 2005, vol. 127, p. 16788.
13. Trifonov, A.A., Spaniol, T.P., and Okuda, J., *Organometallics*, 2001, vol. 20, p. 4869.
14. Panda, T.K., Hrib, C.G., Jones, P.G., et al., *Eur. J. Inorg. Chem.*, 2008, vol. 2008, p. 4270.
15. Jian, Z., Cui, D., Hou, Z., et al., *Chem. Commun.*, 2010, vol. 46, p. 3022.
16. Jian, Z., Tang, S., and Cui, D., *Chem. Eur. J.*, 2010, vol. 16, p. 14007.
17. Rufanov, K.A., Petrov, A.R., Kotov, V.V., et al., *Eur. J. Inorg. Chem.*, 2005, vol. 2005, p. 3805.
18. Jian, Z., Petrov, A.R., Hangaly, N.K., et al., *Organometallics*, 2012, vol. 31, p. 4267.
19. Deng, M., Chi, S.H., and Luo, Y.J., *New J. Chem.*, 2015, vol. 39, p. 7575.
20. Pan, Y.P., Rong, W.F., Jian, Z.B., et al., *Macromolecules*, 2012, vol. 45, p. 1248.
21. Xu, S.T., Wang, J.X., Zhai, J.J., et al., *Organometallics*, 2021, vol. 40, p. 3323.

22. Li, X., Wang, X., Tong, X., et al., *Organometallics*, 2013, vol. 32, p. 1445.
23. Beetstra, D.J., Meetsma, A., Hessen, B., et al., *Organometallics*, 2003, vol. 22, p. 4372.
24. Otero, A., Fernandez-Baeza, J., Antinolo, A., et al., *Organometallics*, 2008, vol. 27, p. 976.
25. Litlabø, R., Enders, M., Törnroos, K.W., et al., *Organometallics*, 2010, vol. 29, p. 2588.
26. Tao, X., Gao, W., Huo, H., et al., *Organometallics*, 2013, vol. 32, p. 1287.
27. Arndt, S., Spaniol, T.P., and Okuda, J., *Organometallics*, 2003, vol. 22, p. 775.
28. Hitzbleck, J. and Okuda, J., *Organometallics*, 2007, vol. 26, p. 3227.
29. Pan, L., Zhang, K., Nishiura, M., et al., *Macromolecules*, 2010, vol. 43, p. 9591.
30. Cheng, J., Cui, D., Chen, W., et al., *J. Organomet. Chem.*, 2002, vol. 658, p. 153.
31. Zhang, L., Zhou, X., Cai, R., et al., *J. Organomet. Chem.*, 2000, vol. 612, p. 176.
32. Li, X., Nishiura, M., Hu, L., et al., *J. Am. Chem. Soc.*, 2009, vol. 131, p. 13870.
33. Zhang, L., Luo, Y., and Hou, Z., *J. Am. Chem. Soc.*, 2005, vol. 127, p. 14562.
34. Wang, B., Wang, D., Cui, D., et al., *Organometallics*, 2007, vol. 26, p. 3167.
35. Wang, B.L., Cui, D.M., and Lv, K., *Macromolecules*, 2008, vol. 41, p. 1983.
36. Zhang, K., Dou, Y.L., Jiang, Y., et al., *Macromolecules*, 2021, vol. 54, p. 9445.
37. Shapiro, P.J., Bunel, E., Schaefer, W.P., et al., *Organometallics*, 1990, vol. 9, p. 867.
38. Liu, D.T., Yao, C.G., Wang, R., et al., *Angew. Chem., Int. Ed.*, 2015, vol. 54, p. 5205.
39. Wang, Z.C., Liu, D.T., and Cui, D.M., *Macromolecules*, 2016, vol. 49, p. 781.
40. Liu, D.T., Wang, M.Y., Wang, Z.C., et al., *Angew. Chem., Int. Ed.*, 2017, vol. 56, p. 2714.
41. Wang, T.T., Liu, D.T., and Cui, D.M., *Macromolecules*, 2019, vol. 52, p. 9555.
42. Wu, Y., Wang, Z.C., Liu, D.T., et al., *Macromolecules*, 2020, vol. 53, p. 8333.
43. Zhong, Y.H., Wu, Y., and Cui, D.M., *Macromolecules*, 2021, vol. 54, p. 1754.
44. Kaneko, H., Nagae, H., Tsurugi, H., et al., *J. Am. Chem. Soc.*, 2011, vol. 133, p. 19626.
45. Altenbuchner, P.T., Adams, F., Kronast, A., et al., *Polym. Chem.*, 2015, vol. 6, p. 6796.
46. Kronast, A., Reiter, D., Altenbuchner, P.T., et al., *Macromolecules*, 2016, vol. 49, p. 6260.
47. Xu, T.Q., Yang, G.W., and Lu, X.B., *ACS Catal.*, 2016, vol. 6, p. 4907.
48. Yang, J., Yu, Y., Qu, J., et al., *Dalton Trans.*, 2017, vol. 46, p. 16993.
49. Li, M., Wang, C.P., Chen, J., et al., *Dalton Trans.*, 2018, vol. 47, p. 15967.
50. Yan, C., Xu, T.Q., and Lu, X.B., *Macromolecules*, 2018, vol. 51, p. 2240.
51. Oishi, M., Yoshimura, R., and Nomura, N., *Inorg. Chem.*, 2019, vol. 58, p. 13755.
52. Zhao, Y., Lu, H., Luo, G., et al., *Catal. Sci. Technol.*, 2019, vol. 9, p. 6227.
53. Zhuang, Q., Mou, Z., Gu, J., et al., *Z. Anorg. Allg. Chem.*, 2020, vol. 646, p. 70.
54. Wang, C.P., Chen, J., Xu, W., et al., *Inorg. Chem.*, 2020, vol. 59, p. 3132.
55. Zhang, X., Zhou, S., Wang, D., et al., *Organometallics*, 2021, vol. 40, p. 3462.
56. Wang, Y., Duan, J.B., Liu, Z.X., et al., *Polym. Chem.*, 2020, vol. 11, p. 3434.
57. Wang, Y., Jiang, H., Wang, H., et al., *J. Rare Earths*, 2022.
https://doi.org/10.1016/j.jre.2022.02.018
58. Lappert, M.F. and Pearce, R., *Chem. Commun.*, 1973, no. 4, p. 126.
59. Wei, Y., Yu, Z., Wang, S., et al., *J. Organomet. Chem.*, 2008, vol. 693, p. 2263.
60. Elvidge, B.R., Arndt, S., Zeimentz, P.M., et al., *Inorg. Chem.*, 2005, vol. 44, p. 6777.
61. Altenbuchner, P.T., Soller, B.S., Kissling, S., et al., *Macromolecules*, 2014, vol. 47, p. 7742.